CHEMISTRY OF LIGHT INTERACTION

CHEMPHOTOCHEM

ACROSS THE WHOLE SPECTRUM

Accepted Article

Title: Hydrostatic Pressure-Controlled Ratiometric Luminescence Responses of Dibenzo[a,j]phenazine-Cored Mechanoluminophore

Authors: Youhei Takeda, Hiroaki Mizuno, Yusuke Okada, Masato Okazaki, Satoshi Minakata, Thomas Penfold, and Gaku Fukuhara

To be cited as: *ChemPhotoChem* 10.1002/cptc.201900190

Link to VoR: http://dx.doi.org/10.1002/cptc.201900190

A Journal of

ChemPubSoc Europe

WILEY-VCH

www.chemphotochem.org

10.1002/cptc.201900190

WILEY-VCH

Hydrostatic Pressure-Controlled Ratiometric Luminescence Responses of Dibenzo[*a,j*]phenazine-Cored Mechanoluminophore

Youhei Takeda,*[a] Hiroaki Mizuno,[b] Yusuke Okada,[b] Masato Okazaki,[a] Satoshi Minakata,[a] Thomas Penfold,*[c] and Gaku Fukuhara*[b,d]

Abstract: Understanding changes to excited state properties under the influence of an external stimuli, such as pressure or temperature, is important in the context of optimizing molecular components for a number of applications including sensors and imaging reagents. Herein, we use UV/vis, fluorescence and excitation spectroscopies, and fluorescence lifetime measurements supported by calculations to probe the effect of hydrostatic pressure on the excited state characteristics of a conformationally-divergent mechanochromic compound in toluene and methylcyclohexane. We demonstrate that hydrostatic pressure can be used to manipulate the equilibria between excited state conformers. This work provides new perspectives for mechanoresponsive materials and as attractive alternative to conventional ratiometric sensors.

Introduction

Luminophores that show ratiometric responses towards various stimuli (e.g., chemicals and intracellular signals) and media conditions (e.g., solvent polarities and viscosities) hold great promise for applications in sensing, probing, and imaging.[1] A well-known family of ratiometric luminophores are the D–A dyads, where an electron-donor (D) and electron-acceptor (A) are connected through a single bond or a vinylene unit. Typically, this type of chromophoric compound shows dual emission in polar solvents: an emission at shorter wavelength from the locally excited (LE) state on either the donor or acceptor and another at longer wavelength arising from the charge-transfer state (CT). For the latter, an excited state geometry change around the linkage usually occurs to increase the dihedral angle between the D and A group, i.e., twisted intramolecular charge-transfer (TICT).[2] Since the rotation of the D and A moieties around the single bond is susceptible to microenvironmental polarity, these D–A dyads serve as viscosity and thermal sensors.[3] On the other hand, an emerging class of ratiometric luminophores include π-conjugated compounds which are bent in their electronic ground state, such as *N,N'*-disubstituted dihydrophenazines (DHPZs)[4] and cyclooctatetraene (COT)-fused acenes.[5] Upon excitation, a remarkable planarization occurs drastically tuning the emission color. As this planarization depends on the environment of the luminophore, such systems are able to measure viscosity, temperature, and membrane tensions.[4,5]

Mechanochromic luminescent (MCL) compounds that show reversible emission color changes in the solid state in response to mechanical forces, heating/cooling, and organic vapors, have rapidly emerged as smart materials over the last decade.[6] In fact, MCL materials are applied to security inks, molecular encryptions, and pressure/thermo-sensors. Importantly, the development of conventional MCL materials is dominated by spontaneous, "molecular-delegated" self-assembly of luminophores which sometimes leads to the formation of multiple metastable emissive states. However, rational approaches to their design have not yet been established. This ultimately limits the variety and contrast of emission colors due to the intrinsic difficulty in rationally predicting the thermodynamic stabilities of the self-assembled molecules in the condensed phases.

In contrast to the conventional approach, we have recently developed thermally activated delayed fluorescence (TADF)-active and multi-color-changing MCL compounds, i.e., **PTZ-DBPHZ** (Figure 1a) and its derivatives, based on the conformationally-dictated regulation mechanism.[7] As related studies, Dias and Grazulevicius also have recently developed TADF-active MCL compounds based on a similar twisted D-A-D scaffold.[8] The **PTZ-DBPHZ** molecule, which has two phenothiazine (PTZ) donor moieties attached to a dibenzo[*a,j*]phenazine (DBPHZ) acceptor.[9] As shown in Figure 1a, **PTZ-DBPHZ** can adopt at least four different conformers in the electronic ground state, which depend on the geometrical arrangement of the PTZ with respect to the acceptor unit: quasi axial-quasi axial (*syn* and *anti*; *ax-ax*), quasi equatorial-quasi axial (*eq-ax*), and quasi equatorial-quasi equatorial (*eq-eq*). Very recently, we have used time-resolved spectroscopy to reveal that the conformational changes in the ground and excited states strongly dictate the photophysical properties of the solid state (Figure 1b).[10] These findings indicate that **PTZ-DBPHZ** is a promising ratiometric luminophore given that the four conformational distributions in solution can be controlled by external stimuli (Figure 1c).

[a] Prof. Dr. Y. Takeda, Dr. M. Okazaki, Prof. Dr. S. Minakata
Department of Applied Chemistry, Graduate School of Engineering
Osaka University
Yamadaoka 2-1, Suita, Osaka 565-0871 (Japan)
E-mail: takeda@chem.eng.osaka-u.ac.jp
[b] H. Mizuno, Y. Okada, Prof. Dr. G. Fukuhara
Department of Chemistry
Tokyo Institute of Technology
2-12-1 Ookayama, Meguro-ku, Tokyo 152-8511 (Japan)
E-mail: gaku@chem.titech.ac.jp
[c] Prof. Dr. T. Penfold
Chemistry School of Natural and Environmental Sciences
New Castle University
Newcastle upon Tyne NE1 7RU (United Kingdom)
E-mail: tom.penfold@newcastle.ac.uk
[d] JST, PRESTO
4-1-8 Honcho, Kawaguchi, Saitama 332-0012 (Japan)

Supporting information for this article is given via a link at the end of the document.

Hydrostatic pressure is the most appropriate control factor for the present study, and indeed solutions of various luminophores under hydrostatic pressure have previously been investigated.[11–19] So far, many sophisticated studies on the effects of hydrostatic pressure on the photophysics of luminophores such as pyrenes,[11,12] 9,9'-bianthryls,[13] 4-(9-anthrylmethyl)-*N,N*-dimethylaniline (AMDMA),[14] (*N,N*-dimethylamino)benzonitrile (DMABN)-type D–A compounds,[15,16] BODIPY derivatives,[17] tryptophan,[18] and fluorescent cyclophane[19] have been examined. In contrast, the effect of hydrostatic pressure on the photophysical properties of MCL compounds in solution has been much less explored, with studies in the solid-state dominating.[20] In the present work, we study the emission properties of **PTZ-DBPHZ** in solution under the influence of hydrostatic pressure. We reveal that under hydrostatically pressurized conditions, unusual but interesting ratiometric luminescence responses observed originate from a ternary emission comprising of an ^{1}LE and two different ^{1}CT excited states associated with different conformers. The present results and concepts proposed herein will provide with deeper mechanistic insights into the factors that control mechanochromism outcomes under high pressure.

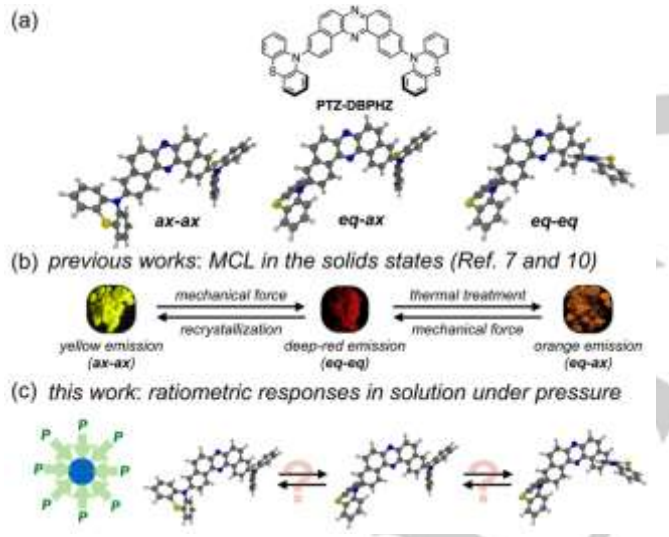

Figure 1. (a) Chemical structure of **PTZ-DBPHZ** and conformers (quasi axial-quasi axial; *ax-ax*, quasi equatorial-quasi axial; *eq-ax*, quasi equatorial-quasi equatorial; *eq-eq*). Schematic illustration for (b) previous works and (c) this work.

Results and Discussion

UV/vis and luminescence spectra of the solution in toluene

The hydrostatic pressure effects on the absorption and luminescence properties of solutions of **PTZ-DBPHZ** were investigated in toluene and methylcyclohexane (MCH) (For the detailed apparatus set-up, see Figure S1 in the supporting information (SI)). Very recently, we have revealed that a toluene solution of **PTZ-DBPHZ** drastically affects the CT band compared to its alkane solution,[7a] indicating that the two solvents are better candidates of the present hydrostatic pressure experiments for the comparison reasons. Alcohols and acetonitrile as polar solvent are inadequate due to the quite poor solubility of **PTZ-DBPHZ**. Therefore, we first examined the concentration effect of **PTZ-DBPHZ** in the two solvents: the UV/vis and fluorescence spectra of the **PTZ-DBPHZ** compound in toluene from 11 μM to 203 μM and in MCH from 17 μM to 99 μM were measured, and the fluorescence maxima (longer wavelength) obtained in the two solvents showed good straight lines against the concentration examined (Figure S2), indicating that **PTZ-DBPHZ** under the concentration conditions examined for all the photophysical investigations in the present study is an isolated state. The three luminescence waveforms from the LE, CT1, and CT2 states (*vide infra*) under the applied pressures examined are separable as common Gaussian curves (Figure S3). The waveform separation spectra gave integral areas, listed in Table S1, to obtain the quantum yield ratios (Φ_{CT}/Φ_{LE}) calculated by division of each area.

The absorption spectrum of the solution of **PTZ-DBPHZ** in toluene as a function of hydrostatic pressure are shown in Figure 2. This spectrum is composed of four distinct bands at 300, 340, 400 and 425 nm and a broader band at approximately 450 nm. Recently, Monkman and co-workers characterize the transitions of the DBPHZ-cored D–A–D triad (D = phenoxazine).[21] The broad absorption in their spectrum was assigned to the pure CT state and the vibronic absorption at around 400 nm was to the π-π* transition of the DBPHZ unit. Consequently, on the basis of this work, we assign the band at 450 nm to a charge transfer (CT) from the PTZ to the DBPHZ. The band at 340 nm corresponds to an LE on the PTZ, while the remaining bands (300, 400 and 425 nm) are associated with an LE state on DBPHZ. As a function of increasing pressure, the first absorption maxima bathochromically shifts from 454 nm at 0.1 MPa to 461 nm at 350 MPa with –0.921 cm^{-1}/MPa (Figure S4a). This is in good agreement with the behavior of well-studied D-A-type luminophores such as *p*-(9-anthryl)-dimethylaniline (ADMA) and 6-propionyl-2-dimethylaminonaphthalene (PRODAN).[15a] It is well-known that increasing pressure causes a significant increase in refractive index[22] and thereby polarizability, which shifts the absorption peaks to lower energy.[23] This shift is accompanied by a monotonic hyperchromic effect (Figure S4b) which is due to the increase in effective concentration upon pressurization.[24]

The population of the *syn* and *anti ax-ax*, *eq-ax*, and *eq-eq* conformers, calculated from a Boltzmann weighting of the relative energy of each conformer simulated using DFT(M062X) under the ambient conditions (0.1 MPa in toluene) is expected to be 3%, 5%, 41%, and 51%, respectively. Importantly, for all of the pressure ranges examined (0.1–350 MPa), the changes in the UV/vis spectra are relatively small (Figure 2a), suggesting little effect of hydrostatic pressure on the relative population of conformers in the electronic ground state. This is consistent with the small changes in the excitation spectra (Figure S6). The pressure-induced

changes in absorption and luminescence spectra are completely reversible.

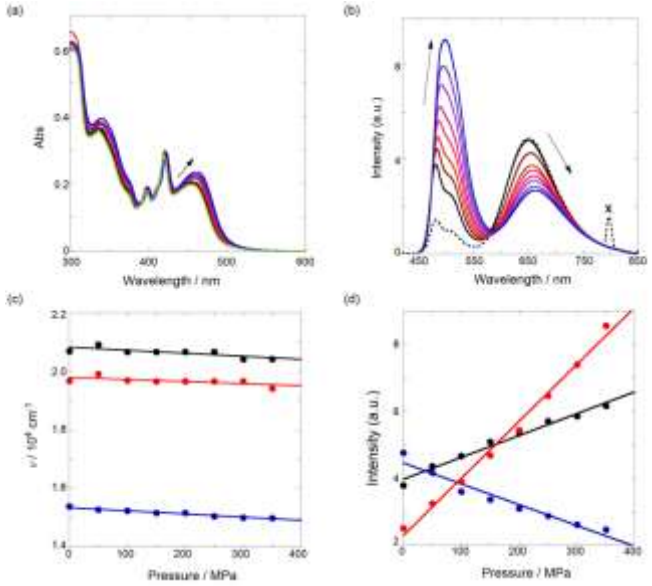

Figure 2. (a) UV/vis spectra and (b) fluorescence spectra (excited at 430 nm) of the solutions of **PTZ-DBPHZ** (222 μM) at 0.1, 50, 100, 150, 200, 250, 300, and 350 MPa (from black to blue) and 0.1 MPa excited at 400 nm (dotted line) and 0.1 MPa depressurized from 350 MPa (light green) in toluene at room temperature, measured in a high-pressure cell. Plots of (c) fluorescence maxima at the LE band (black; correlation coefficient r = 0.797, slope; –1.05 cm^{-1}/MPa), the CT1 band (red; r = 0.691, slope; –0.748 cm^{-1}/MPa), and the CT2 band (blue; r = 0.984, slope; –1.10 cm^{-1}/MPa) and (d) fluorescence changes at 481 nm (black; r = 0.990, slope; 0.00653/MPa), 508 nm (red; r = 0.996, slope; 0.0170/MPa), and 645 nm (blue; r = 0.974, slope; –0.00622/MPa) in toluene as a function of pressure; the three bands, particularly for the LE (408 nm) and CT1 (508 nm), were estimated by the waveform separation spectra (see Figure S3).

The emission spectrum of the solutions of **PTZ-DBPHZ** in toluene is also shown in Figure 2. Under ambient pressure (0.1 MPa), the dilute toluene solution of **PTZ-DBPHZ** showed a ternary emission peaked at 481, 508, and 650 nm (Figures 2b and S3). The emission maximum at 481 nm is slightly blue-shifted to 453 nm (Δν 1290 cm^{-1}) in the less polar MCH solvent (see Figures 5b and S3). In contrast, the emission maxima at 508 and 650 nm are hypsochromically shifted to 468 (Δν 1680 cm^{-1}) and 571 nm (Δν 2130 cm^{-1}) in MCH (Figure 5b). Consequently, the bands at 481, 508, and 650 nm are assigned to the luminescence from the LE and two different CT states (designated as CT1 and CT2), respectively. The LE emission originates from the either **DBPHZ** or **PTZ** moiety of the *ax-ax* conformer, and its position is in good agreement with their emission spectra reported in the literature.[25,26] CT1 and CT2 derive from the *ax-eq* and *eq-eq* conformers, respectively. This assignment is supported by the fluorescence lifetime analyses (see Figure 8, Table S2, and the relevant discussions) and TDDFT(M062X), the latter of which gave the lowest singlet state peaks 452 nm (*ax-eq*), and 692 nm (*eq-eq*), respectively. The orbitals involved in these transitions are shown in the Figure S5.

The luminescence intensity ratio of these emissions excited at 430 nm in toluene does not reflect conformational population-weighted distribution calculated for the absorption spectrum (Figure 2b, the solid black line). Interestingly, upon excitation at 400 nm, the emission spectrum shows a better agreement with the conformer population-weighted distribution (Figure 2b, the dotted black line). When the molecules are excited at lower energy, i.e., 430 nm, all three bands emit equally. However, higher excitation energy (400 nm) leads to a higher degree of excess energy and in this case, predominant formation of the CT excited state is found. This is consistent with previous observations,[27] and we propose that the excess energy enables molecular rearrangement in the excited state.[28]

Most importantly, the emissions (excited at 430 nm) are significantly dependent on the applied pressures and thus show ratiometric responses (Figure 2b). The emission intensity of CT2 (*eq-eq*-like conformation) gradually decreases with increasing pressure, while the intensities of the LE (*ax-ax*-like conformation) and CT1 (*ax-eq*-like conformation) steadily increases (Figure 2b and d). In addition to the intensity changes, the peak maxima bathochromically shift (Figure 2c) as a function of pressure with –1.05 cm^{-1}/MPa for LE, –0.748 cm^{-1}/MPa for CT1, and –1.10 cm^{-1}/MPa for CT2, respectively. This is due to the increase in the dielectric constant of toluene with pressure.[29]

Kinetic processes in the excited states

The kinetic processes for the equilibrium in the excited-states between LE, CT1, and CT2 can be illustrated in Scheme 1. According to the model, the quantum yield ratios (Φ_{CT}/Φ_{LE}) of CT and LE emissions are expressed as Eq. (1) and Eq. (2), where k_1 and k_3 represent the rate constants for the formation of CT1 and CT2 states, respectively, while k_2 and k_4 backward rates to form the LE state. The radiative and non-radiative rates from the LE, CT1, and CT2 states are denoted with k_r^{LE}, k_r^{CT1}, k_r^{CT2}, k_{nr}^{LE}, k_{nr}^{CT1}, and k_n^{rCT2}, respectively. Considering the kinetic processes' equation for only one CT without the other CT against LE may be better for the simplicity.

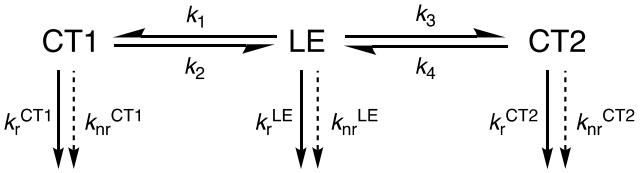

Scheme 1. Kinetic processes of **PTZ-DBPHZ** in solution.

$$\frac{\Phi_{CT1}}{\Phi_{LE}} = \frac{k_r^{CT1} k_1}{k_r^{LE}[k_2 + k_r^{CT1} + k_{nr}^{CT1}]} \quad (1)$$

$$\frac{\Phi_{CT2}}{\Phi_{LE}} = \frac{k_r^{CT2} k_3}{k_r^{LE}[k_4 + k_r^{CT2} + k_{nr}^{CT2}]} \quad (2)$$

To thus elucidate the excited-state behaviors of the ternary emission in toluene, the natural logarithms of the quantum yield ratios ln(Φ_{CT}/Φ_{LE}) were plotted against the pressure as were the cases with previous literatures (Figure 3a).[13–15] Intriguingly, an inflection point at around 200 MPa was observed in the ln(Φ_{CT1}/Φ_{LE}) plot (black circles in Figure 3a). In the lower pressure region, i.e., lower viscosity, at 0.1–200 MPa, the ratio increased monotonically, whereas in the higher-pressure region, i.e., higher viscosity, at 200–350 MPa, it decreased as a function of pressure. This pressure-dependent behavior is likely to be responsible for a dramatic change in kinetics involved in the equilibrium in the excited states such as the shift from thermodynamic control (k_2 >> k_r^{CT1} + k_{nr}^{CT1}: Φ_{CT1}/Φ_{LE} = k_r^{CT1}/k_r^{LE}•K; K = k_1/k_2) to kinetic control (k_2 << k_r^{CT1} + k_{nr}^{CT1}: Φ_{CT1}/Φ_{LE} = (k_r^{CT1}/k_r^{LE})•k_1/(k_r^{CT1} + k_{nr}^{CT1}) = βk_1).[13,14,15d] In contrast, the ratio of ln(Φ_{CT2}/Φ_{LE}) falls on a single straight line through the pressure ranges applied (red circles in Figure 3a), indicating the significant dominance of kinetic control (Φ_{CT2}/Φ_{LE} = β'k_3; β' = (k_r^{CT2}/k_r^{LE})/(k_r^{CT2} + k_{nr}^{CT2})) by increasing the solvent viscosity to suppress the rearrangement of the PTZ donor unit. From the kinetically-controlled regime in Figure 3a, the apparent activation volumes $\Delta V^{\ddagger}_{obs}$ were calculated from the Eq. (3) to be 2.9 cm^3/mol for CT1-LE and 9.3 cm^3/mol for CT2-LE in the excited-state conversions. These positive $\Delta V^{\ddagger}_{obs}$ values, i.e., invalid transition-state theory (TST) regime, for the processes can be reasonably accounted in terms that the aromatic toluene molecules easily solvate to the **PTZ-DBPHZ** molecule, particularly for the *eq-eq*-like conformer (CT2), to form a solvent cluster, and hence such the dynamic solvent effect partly restricts the rearrangement of the donor units under high pressure conditions.[30] Given the free volume limited model under high pressure is adopted,[31] the power low parameter (α) as a fraction of the critical volume required for motion in a viscous solvent can be obtained from the plots of ln(Φ_{CT}/Φ_{LE}) against ln(η) (Figure 3b and Eq. (4)). The α value of 0.69 for CT2-LE quantitatively indicates the degree of rearrangement of the donor unit in the excited-state process.

$$\frac{\partial\, ln(\frac{\Phi_{CT}}{\Phi_{LE}})}{\partial P} = -\frac{\Delta V^{\ddagger}_{obs}}{RT} \quad (3)$$

$$ln(\frac{\Phi_{CT}}{\Phi_{LE}}) = -\alpha\, ln(\eta) + C \quad (4)$$

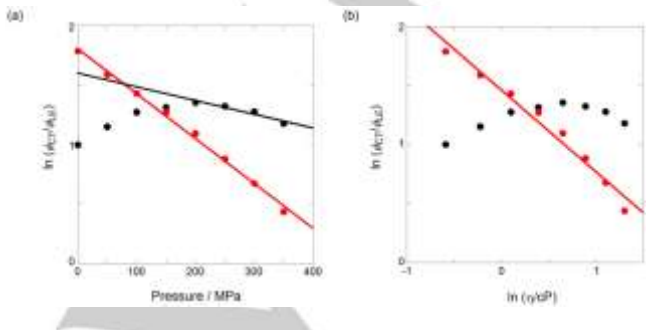

Figure 3. Plots of the natural logarithm of the quantum yield ratios (black; CT1 vs LE, red; CT2 vs LE) against (a) pressure (black; r = 0.963, slope; –0.00116/MPa (≥200 MPa), red; r = 0.998, slope; –0.00377/MPa) and (b) ln(η/cP); pressure-dependent viscosities (η) were estimated by the data described in ref. 29. (red; r = 0.987, slope; 0.69).

It is noted that the emission intensities of LE at 481 and CT1 at 508 nm follow the Förster-Hoffmann equation [log(I) = B log(η) + C] (Figure 4),[32] indicating that **PTZ-DBPHZ** can serve as a viscosity sensor as D-A type molecular rotors.[3] The sensitivity factor (B) as 0.636 for CT1 is larger by a factor of 2.6 than that as 0.248 for LE, reasonably due to the more polarized nature of the excited CT state.

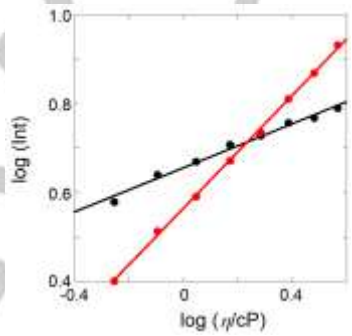

Figure 4. Plot of fluorescence intensities at 481 (black; LE; r = 0.994, B; 0.248, C; 0.656) and 508 nm (red; CT1; r = 0.999, B; 0.636, C; 0.565) according to the Förster-Hoffmann equation for **PTZ-DBPHZ** in toluene; pressure-dependent viscosities (η) were estimated by the data described in ref. 29.

UV/vis and luminescence spectra of the solution in MCH

To further examine the solvent effects on the luminescence properties under high pressure, the spectroscopic measurements of the solution of **PTZ-DBPHZ** in MCH under hydrostatic pressure were performed (Figure 5). The pressurization again did not give a significant influence on the population of conformers in the ground state, which is evident from the slight changes in UV/vis and excitation spectra (Figures 5a and S7).

At the ambient pressure (0.1 MPa), the emission spectrum shows a strong preference for the lowest CT2 transition, which is in part due to the previously discussed excitation wavelength dependence. However, using the DFT (M062X) energies calculated for each conformer, the excited population distribution is expected to be 2%, 3%, 25%, and 70% for the *syn* and *anti* *ax-ax*, *eq-ax*, and *eq-eq* conformations, respectively. This illustrates that the preference for the CT2 emission is also controlled in part by the solvent dependent relative energies of each conformer. This origin for this is the difference in the dipole moment of **PTZ-DBPHZ** of the *eq-ax* and *eq-eq* geometries, which is 5.77 D and 0.66 D, respectively. This means the favorable dipole-dipole interactions will stabilize the *eq-ax* conformer in higher polarity solvents (toluene>MCH).

The peaks are slightly hypsochromically shifted compared to those observed in toluene (*vide supra*), as the consequence of the less polar MCH solvent. As shown in Figure 5c, with

increasing pressure, the peak maxima at the CT bands bathochromically shifted with –0.691 cm^{-1}/MPa for CT1 and –1.29 cm^{-1}/MPa for CT2, respectively, while the LE peak almost did not change with 0.0313 cm^{-1}/MPa. Notably, the emission intensities of all the peaks linearly increased as a function of pressure (Figures 5b and d), the behavior of which is in contrast with the ratiometric responses observed in toluene (Figures 2b and d). The intensity increasing, in particular for CT2, may indicate that the non-radiative deactivation of the excited states is suppressed by the restriction of molecular vibrations associated with the increased viscosity at higher pressure (see discussion for the lifetime analyses).

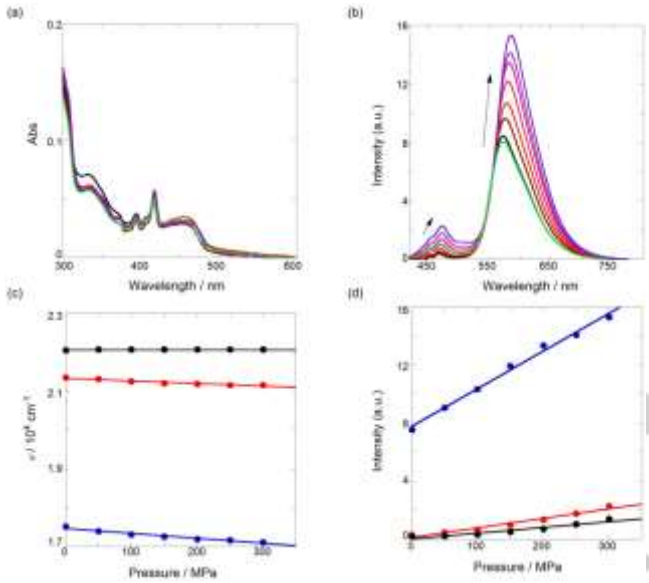

Figure 5. (a) UV/vis spectra and (b) fluorescence spectra (excited at 400 nm) of the solutions of **PTZ-DBPHZ** (126 μM) at 0.1, 50, 100, 150, 200, 250, and 300 MPa (from black to purple) and 0.1 MPa depressurized from 300 MPa (light green) in MCH at room temperature, measured in a high-pressure cell. Plots of (c) fluorescence maxima at LE band (black; r = 0.612, slope; 0.0313 cm^{-1}/MPa), the CT1 band (red; r = 0.959, slope; –0.691 cm^{-1}/MPa), and the CT2 band (blue; r = 0.980, slope; –1.29 cm^{-1}/MPa) and (d) fluorescence changes at 452 nm (black; r = 0.967, slope; 0.00408/MPa), 473 nm (red; r = 0.986, slope; 0.00660/MPa), and 584 nm (blue;r = 0.996, slope; 0.0260/MPa) in MCH as a function of pressure; the three bands were estimated by the waveform separation spectra (see Figure S3).

Therefore, as shown in Figure 6, the natural logarithms of the quantum yield ratios $\ln(\Phi_{CT}/\Phi_{LE})$ of the MCH solutions were plotted against pressure to afford $\Delta V^{\ddagger}_{obs}$ by Eq. (3) as 1.6 cm^3/mol for CT1-LE and 13.1 cm^3/mol for CT2-LE, respectively. Each single straight line indicates that the single mechanism, i.e., the kinetic control, is operative through the whole pressure ranges applied in the present condition. These positive $\Delta V^{\ddagger}_{obs}$ values also indicate the invalid-TST regime, and hence under high pressure conditions even the less-solvating MCH promoted the solvation to the **PTZ-DBPHZ** molecule, particularly for *eq-eq*-like conformer (CT2), based on the relatively large α value by Eq (4) (0.79 for CT2-LE; see Figure S8). As can be seen from Figure 7, all the emission intensities follow the Förster-Hoffmann equation, and the almost same B values as 1.07 for the LE and 1.03 for the CT1 were based on the weak solvation effect of the MCH molecule. The smaller B value of 0.359 for CT2 may be ascribed to the mutual cancelation of the inherent emission quenching by the dynamic solvent fluctuation and of the emission enhancement by the restriction of the molecular vibrations. These observations obtained from the Förster-Hoffmann analyses in toluene and MCH indicate that the **PTZ-DBPHZ** molecule is capable of probing viscosities of solvent with a wide ranges of B values from 0.248 to 1.07 at several wavelengths.

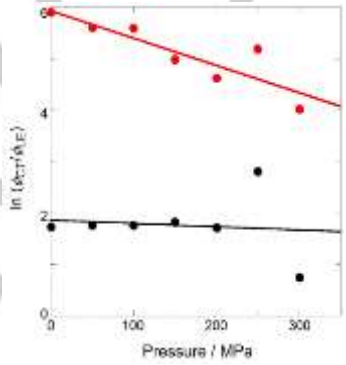

Figure 6. Plot of the natural logarithm of the quantum yield ratios (black; CT1 vs LE, red; CT2 vs LE) against pressure (black; r = 0.120, slope; -0.000656/MPa, red; r = 0.882, slope; -0.00530/MPa).

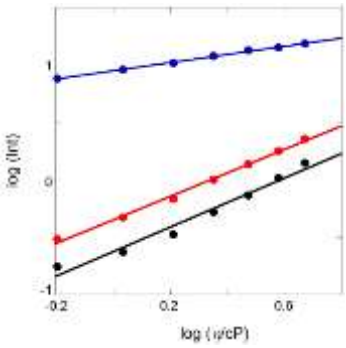

Figure 7. Plot of fluorescence intensities at 452 nm (black; LE; r = 0.986, B; 1.07, C; -0.625), 473 nm (red; CT1; r = 0.998, B; 1.03, C; -0.348), and 584 nm (blue; CT2; r = 0.999, B; 0.359, C; 0.947) according to the Förster-Hoffmann equation for **PTZ-DBPHZ** in MCH; pressure-dependent viscosities (η) were estimated by the data described in ref. 33.

Lifetime measurements upon pressurization

To obtain further insights into the effect of hydrostatic pressure on the luminescent properties of **PTZ-DBPHZ**, time-correlated fluorescence decays were measured under pressurized conditions in nondegassed toluene and MCH (Figure 8) and analyzed by the deconvolution fitting. In toluene, the emission at 490 nm containing the LE and CT1 species decays on the nanosecond timescale throughout the whole

pressure range examined (0.1–350 MPa) (Figure 8a). The fluorescence decay profiles monitored at 490 nm were nicely fitted to a sum of two exponential functions with one very short-lived (τ_1 = 0.1–0.3 ns) and a short-lived (τ_2 = 1.3–1.5 ns) species (for the detailed data, see Table S2). At 0.1 MPa, by shifting the monitored wavelength from 470 to 510 nm, the relative abundance of the very short-lived species (A_1) gradually increased from 25% to 46% with the expense of A_2, indicating that the very short-lived excited species emits at longer wavelength than the short-lived. Therefore, the short-lived species (τ_2) can be assigned to the LE and the very short-lived one (τ_1) to the CT1. The fluorescence decay at 650 nm containing the CT2 species revealed the existence of two components with a long-lived (τ_1 = 10–11 ns) and a relatively long-lived (τ_2 = 79–108 ns) species (Table S2). The long-lived species (τ_1) corresponds to prompt fluorescence from the CT2 state and the relatively long-lived one (τ_2) to the thermally activated delayed fluorescence (TADF) from the same excited state. Although we have revealed that the TADF process is involved in the CT2 state,[7] the quite shortened TADF lifetime decay is highly likely to be responsible for quenching the triplet excited states by oxygen. The most significant observation monitored at 650 nm under high pressure was the steady decreasing A_2/A_1 ratio to eventually reach a single A_1 distribution at 300–350 MPa. This indicates that the increasing viscosity associated with pressure reduces the TADF component of the emission. We propose that pressure restricts the rotation of the donors around the C–N bonds, which significantly decreases the efficiency of the reverse intersystem crossing (rISC) process[34] preventing the TADF process, enabling the present ratiometric responses. On the other hand, the time decay profiles in the MCH solutions were quite different from those observed in toluene (Figures 8c and d). At the ambient pressure, the short-lived species (τ_2: 1.2–1.3 ns) can also be assignable to the LE and the very short-lived one (τ_1: 0.1–0.2 ns) to the CT1 in the same manner. The A_2/A_1 ratio monitored at 460 nm increased as the pressure elevated (Table S2). Interestingly, the A_2/A_1 ratio monitored at 570 nm (τ_1 = 14–30 ns for the CT2; τ_2 = 90–131 ns for the TADF) remains almost constant (6.14–6.69) throughout the whole pressure ranges studied (Table S2). The mutual elongation of the two lifetimes in higher pressure may be explained by the slower ISC/rISC processes, which should be caused by the larger ΔE_{ST} gap due to the destabilization of the ^{1}CT excited states in non-polar solvent.[34] Eventually, the pressure-dependent fluorescence decay profiles monitored at longer wavelength containing the CT2 species in toluene and MCH (Figures 8b and d) show the quite contrasting behaviors: *ratiometric* vs monotonic increase responses.

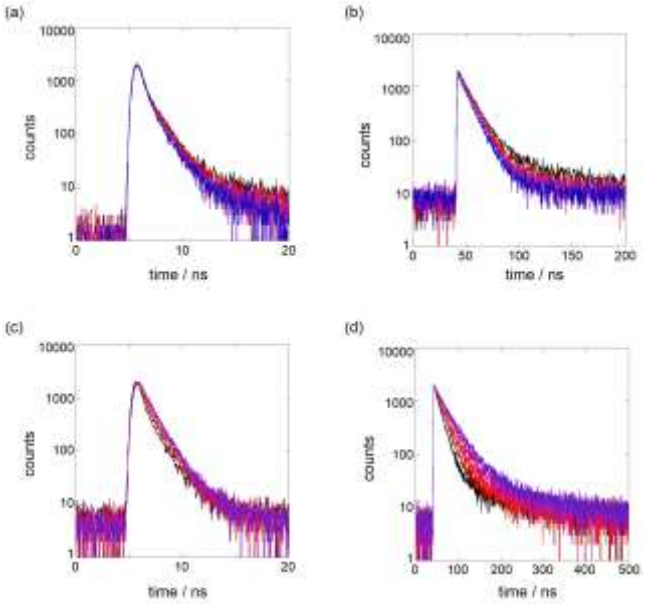

Figure 8. Time-correlated fluorescence decays of the solutions of **PTZ-DBPHZ** in nondegassed toluene (203 μM) monitored at (a) 490 and (b) 650 nm at 0.1, 50, 100, 150, 200, 250, 300, and 350 MPa (from black to blue) and in nondegassed MCH (99 μM) monitored at (c) 460 and (d) 570 nm at 0.1, 50, 100, 150, 200, 250, and 300 MPa (from black to purple) at room temperature, measured in a high-pressure cell.

Mechanistic perspective

On the basis of the results obtained from the steady-state spectroscopies, time-correlated lifetime decay measurements and calculations, in this section we discuss the pressure dependent emission of **PTZ-DBPHZ** and propose a mechanism for the dynamic interchange of the conformers in the ground state and excited states. This is shown schematically in Figure 9.

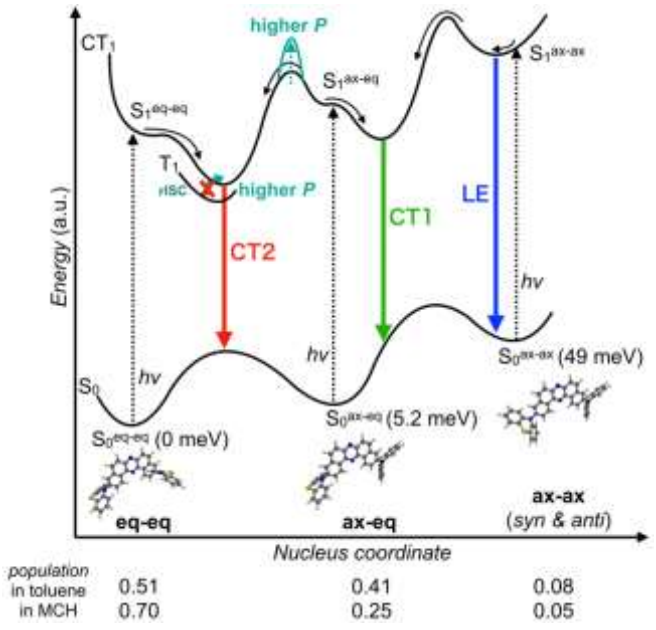

Figure 9. Illustrative diagram of the ground state and excited states of **PTZ-DBPHZ** in toluene. The values in parentheses indicate the relative energies of the *ax-eq* and *ax-ax* conformers in the ground states, compared with the *eq-eq* conformer.

Our density functional calculations have identified four distinct conformers *ax-eq, ax-ax (syn* and *anti),* and *eq-eq*. Using a Boltzmann weight, these are expected to be present in a ratio of 0.41:0.03:0.05:0.51 in toluene and 0.25:0.02:0.03:0.70 in MCH. The *ax-eq* and *eq-eq* dominate and consequently the *ax-ax* conformers are not discussed in the following interpretation. The experimental absorption spectra, shown Figures 2a and 5a, indicate that the population of each conformer is not strongly influenced by pressure, as minimal changes in the UV/vis spectra for both solvents are observed under high pressure. At ambient pressure, these molecules can interconvert in the excited states. This is most clearly seen for **PTZ-DBPHZ** in toluene (Figure 2), as the *eq-eq* emission occurring at 650 nm (Figure 2b) dominants, despite not being the largest conformer in the electronic ground state. This interconversion is consistent with similar effects observed in related D-A luminophores[35] and occurs due to the small barrier between the conformers in the excited state. The ambient pressure emission spectrum in MCH is also dominated by the emission associated with the CT state of the *eq-eq* conformer. However, while the excited wavelength contributes to this, the prominence of the CT state of the solution in MCH is also associated with the relative conformational stability in the electronic ground state, which is why a loss in this emission is not seen with increasing pressure which restricts the conformational reorganization. The origin for this is the difference in the dipole moments of the *eq-eq* (0.66 D) and *eq-ax* (5.77 D) conformers of **PTZ-DBPHZ**. This means that favorable dipole-dipole interactions will stabilize the *eq-ax* conformer in higher polarity solvents. While the small dipole moments of MCH (0.00 D) and toluene (0.36 D) means this will only be a small change, the small energy difference between the states is sufficient to mean that when such interactions are absent, as in MCH, the *eq-eq* conformer is preferred, but in toluene both conformers are present in almost equal quantities.

Upon the application of hydrostatic pressure, the emission spectrum of the solution of **PTZ-DBHZ** in toluene demonstrates how the interconversion between the conformers can be controlled. At a higher pressure, the higher viscosity, i.e., dynamic solvent fluctuation based on the $\Delta V^{\ddagger}_{obs}$, restricts the rotation of the donor units around the C–N bond to increase the barrier for interconversion from the Franck-Condon state generated and consequently a larger contribution from the *ax-eq* conformers is observed. In contrast, for MCH, the higher excitation energy favors the CT2 emission and therefore only an increase in the intensity of all emission peaks is observed. Consequently, in this case, changes in the emission with pressure are predominately reduction of the non-radiative pathways.

Conclusions

In conclusion, for the first time we have revealed the effects of hydrostatic pressure on the photophysical properties of an MCL material **PTZ-DBPHZ** in toluene and MCH solutions. The MCL luminophore in toluene solution showed distinct ratiometric luminescence responses controlled by hydrostatic pressure, which is in quite contrast with the standard emission increasing observed in MCH followed by the Förster-Hoffmann behavior. Importantly, these results demonstrate that the features of mechanochromic compounds upon hydrostatically pressurized conditions can be controlled by simply changing the solvent, which are very different from other D-A chromophores. The present study not only elucidates the factors and mechanisms operative in the hydrostatic pressure-controlled luminescence ratiometric responses but also provides a novel concept for mechanoresponsive materials and an attractive alternative to the conventional ratiometric sensors. To understand the essence of material design for regulating solution-state photophysical properties upon hydrostatically pressurization, further studies on the hydrostatic pressure effect on other MCL materials may be demonstrated in the future.

Experimental Section

General

UV/vis and fluorescence spectra were recorded on JASCO V-560 and FP-8500 spectrophotometers. Fluorescence lifetimes were determined by a Hamamatsu Quantaurus-Tau single-photon-counting apparatus fitted with an LED light source (excitation wavelength: 405 nm).

Materials

Fluorescence-free toluene and MCH were used for spectroscopy without further purification.

Measurements under hydrostatic pressure

All spectroscopic experiments under high pressure were performed by means of a custom-built high-pressure apparatus. The details were described previously.[30] Concisely, a quartz cell with an inner dimension 3 mm (W) x 2 mm (D) x 7 mm (H) linked to a short Teflon tube. A solution was filled up and then the top end was stoppered. The quartz cell containing the sample solution was placed in the pressure apparatus, which was fixed in the spectrometers. The sample solution was set at varying pressures from 0.1 to 350 MPa. The apparatus consists of three optical windows of sapphire for UV/vis and fluorescence spectroscopy and fluorescence lifetime measurement, manufactured by Teramecs Co., Kyoto, Japan.

Computational details

The ground and S_1 state geometries of all four conformers were calculated using density functional theory (DFT) and time dependent density functional theory (TDDFT), respectively. For the ground state a Polarizable Continuum Model (PCM) with the properties of toluene or MCH was used. For the excited states,

the effect of solvation on the emission energy was incorporated using a state-specific polarizable continuum solvation model (SS-PCM).[36,37] All DFT and TDDFT calculations used the functional M062X,[38] the basis set Def2SVP,[38,39] within the Gaussian09 quantum chemistry package.[40]

Acknowledgements

This research was supported by JSPS KAKENHI Grant No. JP 17H05155 (the Grant-in-Aid for Scientific Research on Innovative Areas "π-System Figuration: Control of Electron and Structural Dynamism for Innovative Functions" for Y.T. and No. 19H02746 (Grant-in-Aid for Scientific Research (B)) for G.F. Y.T. acknowledges the financial supports from the Iketani Science and Technology Foundation, and the Continuation Grants for Young Researchers from the Asahi Glass Foundation. G.F. also appreciates the generous support by Japan Science Technology Agency (JST), PRESTO (No. JPMJPR17PA). T.J.P gratefully acknowledges support from the EPSRC through grants EP/N028511/1, EP/R021503/1 and EP/P012388/1.

Conflict of interest

The authors declare no conflict of interest.

Keywords: mechanochromic luminophore • hydrostatic pressure • spectroscopy • delayed fluorescence • conformers

[1] For the reviews on ratiometric probes and imaging agents, see: a) M. H. Lee, J. S. Kim, J. L. Seesler, *Chem. Soc. Rev.* **2015**, *44*, 4185–4191; b) P. Wu, X. Hou, J.-J. Xu, H.-Y. Chen, *Nanoscale* **2016**, *8*, 8427–8442; c) A. S. Klymchenko, *Acc. Chem. Res.* **2017**, *50*, 366–375; d) X. Huang, J. Song, B. C. Yung, X. Huang, Y. Xiong, X. Chen, *Chem. Soc. Rev.* **2018**, *47*, 2873–2920.

[2] For the reviews on TICT phenomena, see: a) W. Rettig, *Angew. Chem. Int. Ed.* **1986**, *25*, 971–988; *Angew. Chem.* **1986**, *98*, 969–986; b) Z. R. Grabowski, K. Rotkiewicz, W. Rettig, *Chem. Rev.* **2003**, *103*, 3899–4031.

[3] For the reviews on viscosity sensors, see: a) M. A. Haidekker, E. A. Theodorakis, *Org. Biomol. Chem.* **2007**, *5*, 1669–1678; b) S.-C. Lee, J. Heo, H. C. Woo, J.-A. Lee, Y. H. Seo, C.-L. Lee, S. Kim, O.-P. Kwon, *Chem. Eur. J.* **2018**, *24*, 13706–13718.

[4] a) Z. Zhang, Y.-S. Wu, K.-C. Tang, C.-L. Chen, J.-W. Ho, J. Su, H. Tian, P.-T. Chou, *J. Am. Chem. Soc.* **2015**, *137*, 8509–8520; b) J. Chen, Y. Wu, X. Wang, Z. Yu, H. Tian, J. Yao, H. Fu, *Phys. Chem. Chem. Phys.* **2015**, *17*, 27658–27664; c) W. Chen, C.-L. Chen, Z. Zhang, Y.-A. Chen, W.-C. Chao, J. Su, H. Tian, P.-T. Chou, *J. Am. Chem. Soc.* **2017**, *139*, 1636–1644; d) G. Sun, H. Zhou, Y. Liu, Y. Li, Z. Zhang, J. Mei, J. Su, *ACS Appl. Mater. Interfaces* **2018**, *10*, 20205–20212; e) Z. Zhang, C.-L. Chen, Y.-A. Chen, Y.-C. Wei, J. Su, H. Tian, P.-T. Chou, *Angew. Chem. Int. Ed.* **2018**, *57*, 9880–9884; *Angew. Chem.* **2018**, *130*, 10028–10032; f) H. V. Humeniuk, A. Rosspeintner, G. Licari, V. Kilin, L. Bonacina, E. Vauthey, N. Sakai, S. Matile, *Angew. Chem. Int. Ed.* **2018**, *57*, 10559–10563; *Angew. Chem.* **2018**, *130*, 10719–10723.

[5] a) C. Yuan, S. Saito, C. Camacho, S. Irle, I. Hisaki, S. Yamaguchi, *J. Am. Chem. Soc.* **2013**, *135*, 8842–8845; b) C. Yuan, S. Saito, C. Camacho, T. Kowalczyk, S. Irle, S. Yamaguchi, *Chem. Eur. J.* **2014**, *20*, 2193–2200; c) S. Saito, S. Nobusue, E. Tsuzaka, C. Yuan, C. Mori, M. Hara, T. Seki, C. Camacho, S. Irle, S. Yamaguchi, *Nat. Commun.* **2016**, *7*, 12094/1–7; d) R. Kotani, H. Sotome, H. Okajima, S. Yokoyama, Y. Nakaike, A. Kashiwagi, C. Mori, Y. Nakada, S. Yamaguchi, A. Osuka, A. Sakamoto, H. Miyasaka, S. Saito, *J. Mater. Chem. C* **2017**, *5*, 5248–5256; e) M. Hada, S. Saito, S. Tanaka, R. Sato, M. Yoshimura, K. Mouri, K. Matsuo, S. Yamaguchi, M. Hara, Y. Hayashi, F. Röhricht, R. Herge, Y. Shigeta, K. Onda, R. J. D. Miller, *J. Am. Chem. Soc.* **2017**, *139*, 15792–15800; f) T. Yamakado, S, Takahashi, K. Watanabe, Y. Matsumoto, A. Osuka, S. Saito, *Angew. Chem. Int. Ed.* **2018**, *57*, 5438–5443; *Angew. Chem.* **2018**, *130*, 5536–5541; g) T. Yamakado, K. Osubo, A. Osuka, S. Saito, *J. Am. Chem. Soc.* **2018**, *140*, 6245–6248.

[6] For the reviews on MCL materials, see: a) Y. Sagara, T. Kato, *Nat. Chem.* **2009**, *1*, 605–610; b) A. Pucci, R. Bizzrri, G. Ruggeri, *Soft Matter*, **2011**, *7*, 3689–3700; c) Z. Chi, X. Zhang, B. Xu, X. Zhou, C. Ma, Y. Zhang, S. Liu, J. Xu, *Chem. Soc. Rev*. **2012**, *41*, 3878–3896; d) Z. Ma, Z. Wang, M. Teng, Z. Xu, X. Jia, *ChemPhysChem* **2015**, *16*, 1811–1828; e) Y. Sagara, S. Yamane, M. Mitani, C. Weder, T. Kato, *Adv. Mater.* **2016**, *28*, 1073–1095; f) S. Xue, X. Qiu, Q. Sun, W. Yang, *J. Mater. Chem. C* **2016**, *4*, 1568–1578; g) P. Xue, J. Ding, P. Wang, R. Lu, *J. Mater. Chem. C* **2016**, *4*, 6688–6706; h) C. Wang, Z. Li, *Mater. Chem. Front.* **2017**, *1*, 2174–2194.

[7] a) M. Okazaki, Y. Takeda, P. Data, P. Pander, H. Higginbotham, A. P. Monkman, S. Minakata, *Chem. Sci.* **2017**, *8*, 2677–2686; b) Y. Takeda, T. Kaihara, M. Okazaki, H. Higginbotham, P. Data, N. Tohnai, S. Minakata, *Chem. Commun.* **2018**, *54*, 6847–6850.

[8] a) R. Pashazadeh, P. Pander, A. Bucinskas, P. J. Skabara, F. B. Dias, J. V. Grazulevicius, *Chem. Commun.* **2018**, *54*, 13857–13860; b) R. Pashazadeh, P. Pander, A. Lazauskas, F. B. Dias, J. V. Grazulevicius, *J. Phys. Chem. Lett.* **2018**, *9*, 1172–1177.

[9] Y. Takeda, M. Okazaki, S. Minakata, *Chem. Commun.* **2014**, *50*, 10291–10294.

[10] P. Data, M. Okazaki, S. Minakata, Y. Takeda, *J. Mater. Chem. C* **2019**, *7*, 6616–6621.

[11] P. C. Johnson, H. W. Offen, *J. Chem. Phys.* **1972**, *56*, 1638–1642.

[12] a) K. Hara, H. Yano, *J. Phys. Chem.* **1986**, *90*, 4265–4268; b) K. Hara, H. Yano, *J. Am. Chem. Soc*. **1988**, *110*, 1911–1915.

[13] a) K. Hara, T. Arase, J. Osugi, *J. Am. Chem. Soc.* **1984**, *106*, 1968–1972; b) K. Hara, T. Arase, *Chem. Phys. Lett.* **1984**, *2*, 178–180; c) K. Hara, *Physica B+C* **1986**, *139 & 140B*, 705–708.

[14] K. Hara, K. Obara, *Chem. Phys. Lett.* **1985**, *117*, 96–98.

[15] a) A. M. Rollinson, H. G. Drickamer, *J. Chem. Phys*. **1980**, *73*, 5981–5996; b) K. Hara, H. Suzuki, *Chem. Phys. Lett*. **1988**, *145*, 269–272; c) K. Hara, W. Rettig, *J. Phys. Chem*. **1992**, *96*, 8307–8309; d) D. S. Burlgarevich, O. Kajimoto, K. Hara, *J. Phys. Chem.* **1995**, *99*, 13356–13361; e) K. Hara, N. Kometani, O. Kajimoto, *J. Phys. Chem.* **1996**, *100*, 1488–1493.

[16] W. Rettig, E. Gilabert, C. Rulliére, *Chem. Phys. Lett*. **1994**, *229*, 127–133.

[17] M. A. H. Alamiry, A. C. Benniston, G. Copley, K. J. Elliott, A. Harriman, B. Steward, Y.-G. Zhi, *Chem. Mater.* **2008**, *20*, 4024–4032.

[18] K. Ruan, S. Tian, R. Lange, C. Balny, *Biochem. Biophys. Res. Commun.* **2000**, *269*, 681–686.

[19] Y. Sagara, N. Tamaoki, G. Fukuhara, *ChemPhotoChem* **2018**, *2*, 959–963.

[20] a) Y. Dong, B. Xu, J. Zhang, X. Tan, L. Wang, J. Chen, H. Lv, S. Wen, B. Li, L. Ye, B. Zou, W. Tian, *Angew. Chem. Int. Ed.* **2012**, *51*, 10782–10785; *Angew. Chem.* **2012**, *124*, 10940–10943; b) K. Nagura, S. Saito, H. Yusa, H. Yamawaki, H. Fujihisa, H. Sato, Y. Shimoikeda, S. Yamaguchi, *J. Am. Chem. Soc.* **2013**, *135*, 10322–10325; c) J. Wu, J. Tang, H. Wang, W. Xu, *J. Phys. Chem. A* **2015**, *119*, 9218–9224; d) C. Feng, K. Wang, Y. Xu, L. Liu, B. Zou, P. Lu, *Chem. Commun.* **2016**, *52*, 3836–3839; e) Y. Zhang, J. Zhang, J. Shen, J. Sun, K. Wang, Z. Xie, H. Gao, B. Zou, *Adv. Opt. Mater*. **2018**, *6*, 1800956; f) Y. Liu, Q. Zeng, B. Zou, Y. Liu, B. Xu, W. Tian, *Angew. Chem. Int. Ed.* **2018**, *57*, 15670–

15674; *Angew. Chem.* **2018**, *130*, 15896–15900; g) J. Wang, A. Li, S. Xu, B. Li, C. Song, Y. Geng, N. Chu, J. He, W. Xu, *J. Mater. Chem. C* **2018**, *6*, 8958–8965; h) J. Xiong, K. Wang, Z. Yao, B. Zou, J. Xu, X.-H. Bu, *ACS Appl. Mater. Interfaces* **2018**, *10*, 5819–5827.

[21] D. de Sa Pereira, C. Menelaou, A. Danos, C. Marian, A. P. Monkman, *J. Phys. Chem. Lett.* **2019**, *10*, 3205–3211.

[22] T. Takagi, H. Teranishi, *J. Chem. Eng. Data* **1982**, *27*, 16–18.

[23] F. A. Bovey, S. S. Yanari, *Nature* **1960**, *186*, 1042–1044.

[24] W. W. Robertson, *J. Chem. Phys*. **1960**, *33*, 362–365.

[25] a) Y. Takeda, M. Okazaki, S. Minakata, *Chem. Commun*. **2014**, *50*, 10291–10294; b) P. Data, P. Pander, M. Okazaki, Y. Takeda, S. Minakata, A. P. Monkman, *Angew. Chem. Int. Ed.* **2016**, *55*, 5739–5744; *Angew. Chem.* **2016**, *128*, 5833–5838.

[26] F. B. Dias, J. Santos, D. R. Graves, P. Data, R. S. Nobuyasu, M. A. Fox, A. S. Batsanov, T. Palmeira, M. N. Berberan-Santos, M. R. Bryce, A. P. Monkman, *Adv. Sci.* **2016**, *3*, 160080.

[27] P. L. dos Santos, J. S. Ward, A. S. Batsanov, M. R. Bryce, A. P. Monkman, *J. Phys. Chem. C* **2017**, *121*, 16462–16469.

[28] D.-G. Chen, T.-C. Lin, Y.-A. Chen, Y.-H. Chen, T.-C. Lin, Y.-T. Chen, P.-T. Chou, *J. Phys. Chem. C* **2018**, *122*, 12215–12221.

[29] F. J. Vieira, C. A. N. de Castro, *Int. J. Thermophys.* **1997**, *18*, 367–378.

[30] A. J. L. Ayitou, G. Fukuhara, E. Kumarasamy, Y. Inoue, J. Sivaguru, *Chem. Eur. J.* **2013**, *19*, 4327–4334.

[31] a) G. E. Johnson, *J. Chem. Phys*. **1975**, *63*, 4047–4053; b) T. Asano, H. Furuta, H. Sumi, *J. Am. Chem. Soc.* **1994**, *116*, 5545–5550.

[32] T. Förster, G. Hoffmann, *Z. Phys. Chem. Neue Folge* **1971**, *75*, 63–76.

[33] A. Baylaucq, C. Boned, P. Dauge, B. Lagourette, *Int. J. Thermophys.* **1997**, *18*, 3–23.

[34] a) J. Gibson, A. P. Monkman, T. J. Penfold, *ChemPhysChem* **2016**, *17*, 2956–2961; b) M. K. Etherington, J. Gibson, H. F. Higginbotham, T. J. Penfold, A. P. Monkman, *Nat. Commun.* **2016**, *7*, 13680; c) J. Gibson, T. J. Penfold, *Phys. Chem. Chem. Phys.* **2016**, *19*, 8428–8434.

[35] a) T. J. Penfold, F. B. Dias, A. P. Monkman, *Chem. Commun.* **2018**, *54*, 3926–3935; b) J. S. Ward, R. S. Nobuyasu, M. A. Fox, A. S. Batsanov, J. Santos, F. B. Dias, M. R. Bryce, *J. Org. Chem.* **2018**, *83*, 14431–14442.

[36] J.-M. Mewes, Z.-Q. You, M. Wormit, T. Kriesche, J. M. Herbert, A. Dreuw, *J. Phys. Chem. A* **2015**, *119*, 5446–5464.

[37] J.-M. Mewes, J. M. Herbert, A. Dreuw, *Phys. Chem. Chem. Phys.* **2017**, *19*, 1644–1654.

[38] Y. Zhao, D. G. Truhlar, *Theor. Chem. Acc.* **2008**, *120*, 215–241.

[39] F. Weigend, R. Ahlrichs, *Phys. Chem. Chem. Phys.* **2005**, *7*, 3297–3305.

[40] F. Weigend, *Phys. Chem. Chem. Phys.* **2006**, *8*, 1057–1065.

FULL PAPER

A conformationally-divergent mechanochromic compound exhibited hydrostatic pressure-controlled ratiometric luminescence responses on the basis of an inhibition of a thermally-activated delayed fluorescence (TADF) process.

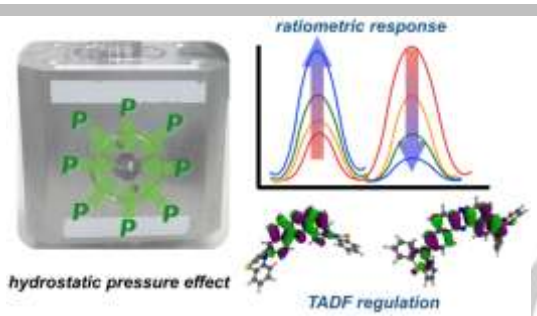

Y. Takeda, H. Mizuno, Y. Okada, M. Okazaki, S. Minakata, T. Penfold,* G. Fukuhara**

Page No. – Page No.

Hydrostatic Pressure-Controlled Ratiometric Luminescence Responses of Dibenzo[*a,j*]phenazine-Cored Mechanoluminophore